

## ARTICLE

# Immunogenicity of self tumor associated proteins is enhanced through protein truncation

Tim Kottke<sup>1</sup>, Kevin G Shim<sup>1,2</sup>, Vanesa Alonso-Camino<sup>1</sup>, Shane Zaidi<sup>1</sup>, Rosa Maria Diaz<sup>1</sup>, Jose Pulido<sup>1,3</sup>, Jill Thompson<sup>1</sup>, Karishma R Rajani<sup>1</sup>, Laura Evgin<sup>1</sup>, Elizabeth Ilett<sup>4</sup>, Hardev Pandha<sup>5</sup>, Kevin Harrington<sup>6</sup>, Peter Selby<sup>4</sup>, Alan Melcher<sup>6</sup> and Richard Vile<sup>1,2,4</sup>

We showed previously that therapy with Vesicular Stomatitis Virus (VSV) expressing tumor-associated proteins eradicates established tumors. We show here that when cellular cDNA were cloned into VSV which retained their own poly-A signal, viral species emerged in culture which had deleted the cellular poly-A signal and also contained a truncated form of the protein coding sequence. Typically, the truncation occurred such that a Tyrosine-encoding codon was converted into a STOP codon. We believe that the truncation of tumor-associated proteins expressed from VSV in this way occurred to preserve the ability of the virus to replicate efficiently. Truncated cDNA expressed from VSV were significantly more effective than full length cDNA in treating established tumors. Moreover, tumor therapy with truncated cDNA was completely abolished by depletion of CD4+ T cells, whereas therapy with full length cDNA was CD8+ T cell dependent. These data show that the type/potency of antitumor immune responses against self-tumor-associated proteins can be manipulated *in vivo* through the nature of the self protein (full length or truncated). Therefore, in addition to generation of neoantigens through sequence mutation, immunological tolerance against self-tumor-associated proteins can be broken through manipulation of protein integrity, allowing for rational design of better self-immunogens for cancer immunotherapy.

*Molecular Therapy — Oncolytics* (2016) **3**, 16030; doi:10.1038/mto.2016.30; published online 7 December 2016

## INTRODUCTION

Immunotherapy for cancer has recently had several notable successes in the context of both antigen specific,<sup>1,2</sup> and antigen non-specific,<sup>3</sup> strategies. Such approaches rely upon the existence of tumor-associated proteins (TAP), against which T cell responses can be raised.<sup>4,5</sup> In most cases, antitumor T cell responses require tolerance to self, or near self, proteins to be broken. Self-TAP may become immunogenic through overexpression, reactivation of expression, or abnormal processing on the target tumor cells.<sup>4</sup> Alternatively, novel immunogenic epitopes, potentially unique to each individual tumor, may be generated within otherwise self-TAP through translocations or by mutation.<sup>5,6</sup> In times of cellular stress, such as infection, the proinflammatory Unfolded Protein Response (UPR) may also play a role in increased processing of abnormal or aberrantly folded proteins.<sup>7–10</sup> For example, ER stress is closely tied to levels of MHC Class I/II expression (reviewed in ref. 11). In addition, activation of the UPR through PERK-eIF2, can favor the translation of cryptic antigens which derive from initiation through CUG codons.<sup>12</sup> Overall, activation of the UPR by both viral infection and by generation of abnormally folded proteins can result in the presentation of an altered repertoire of antigens.

Even when T cells are present which can recognize self, or near self-TAP, tumors evolve rapidly away from the resultant immune pressure to generate antigen loss variants.<sup>13,14</sup> Therefore, we and others have developed immunotherapies which seek to raise T cell responses against multiple antigens simultaneously.<sup>13,15,16</sup> This strategy is based upon the premise that no single cancer cell will be able to evade a multispecific T cell response. In this respect, mice treated with the highly immunogenic platform of the Vesicular Stomatitis Virus (VSV) expressing a TAP cDNA library generated a CD4+ T cell dependent response against several different self-TAP, which, in combination, eradicated well-established tumors.<sup>15,16</sup> Antitumor therapy was immune-mediated following systemic (intravenous) delivery of the library, and was effective against various different histological types of tumor using cDNA from the appropriate tissue source.<sup>15–18</sup> In the case of a melanoma-derived VSV-cDNA library, a combination of 3 individual VSV - VSV-N-RAS, VSV-Cytochrome-C, and VSV-TYRP-1 (VSV-TAP)-treated established subcutaneous B16 melanomas in C57BL/6 mice, almost as effectively as the overall, unfractionated VSV-cDNA library.<sup>16,17</sup> This was associated with a CD4+ T cell dependent IL-17 response to B16 tumor cells but no detectable IFN- $\gamma$  response.<sup>16,17</sup>

The first two authors contributed equally to this work.

<sup>1</sup>Department of Molecular Medicine, Mayo Clinic, Rochester, Minnesota, USA; <sup>2</sup>Department of Immunology, Mayo Clinic, Rochester, Minnesota, USA; <sup>3</sup>Department of Ophthalmology, Mayo Clinic, Rochester, Minnesota, USA; <sup>4</sup>Cancer Research UK Clinical Center, St. James' University Hospital, Leeds, UK; <sup>5</sup>University of Surrey, Guildford, UK; <sup>6</sup>The Institute of Cancer Research, London, UK. Correspondence: R Vile (vile.richard@mayo.edu)

Received 7 October 2016; accepted 15 October 2016

In this study, we further characterized the cDNA inserts of this individual VSV-TAP<sup>16</sup> to understand the mechanisms by which cumulatively they generate antitumor T cell responses. Interestingly, each of the TAPs encoded by the VSV were truncated, but not mutated. When combined, the VSVs expressing full-length cDNAs induced a CD8-dependent antitumor response, while VSVs expressing truncated cDNA generated a

CD4+ T cell dependent antitumor immune response. These data are highly significant for designing better immunogens based on self-TAP for cancer immunotherapy. In addition they may help to explain the etiology of infectious and autoimmune diseases, in which pathogenic infection and/or cellular stress, cause the aberrant folding of normal cellular proteins, leading to the generation of anti-self autoimmunity.<sup>19-22</sup>

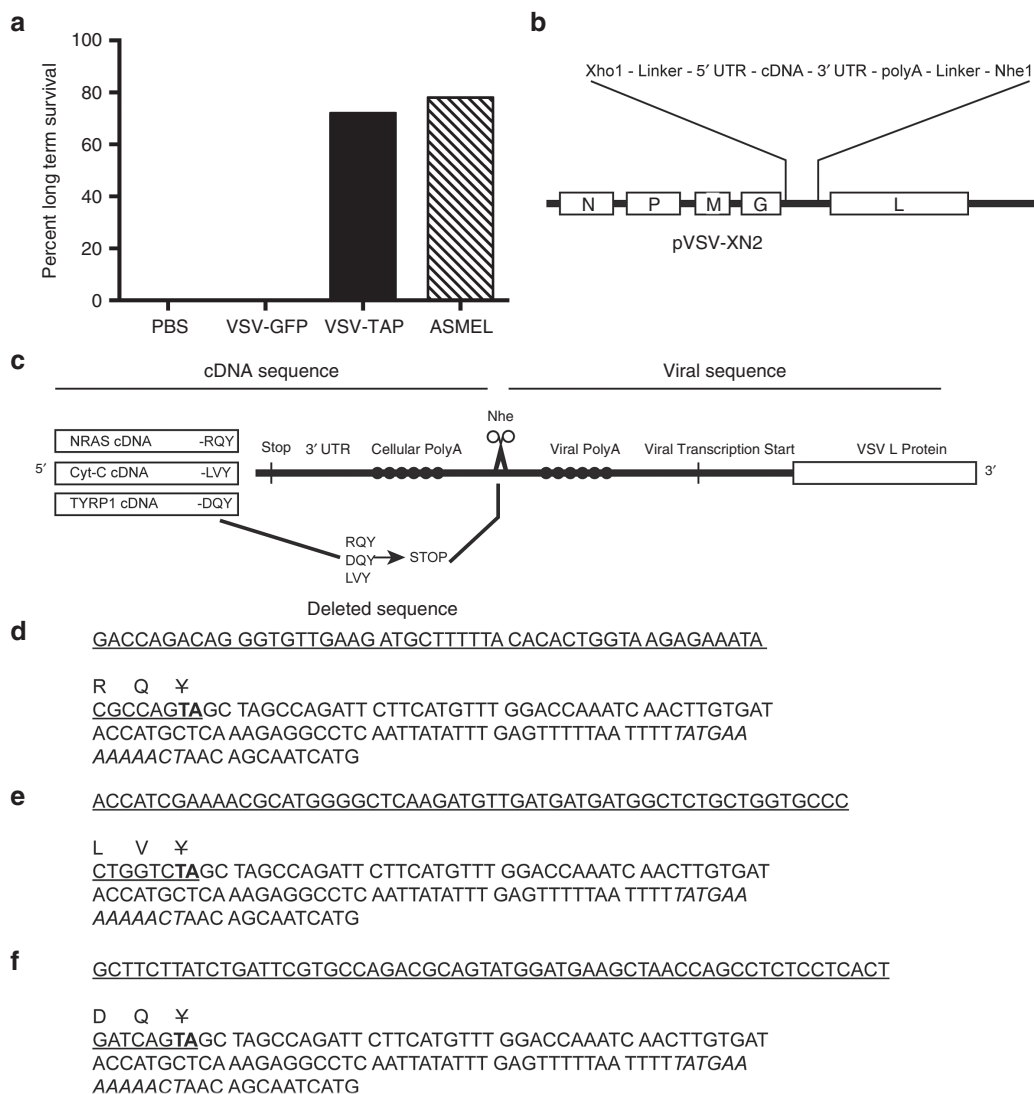


**Figure 1** Immunologically active VSV-TAP are deleted at the 3' ends of the inserted cDNA. **(a)** Mice bearing 5-day-old s.c. B16 tumors were treated ( $n = 7-8$ /group) with nine i.v. injections on days 6-8, 13-15, and 20-22 with: a three-way combination (total viral dose  $10^7$  pfu/injection;  $3 \times 10^6$  pfu of each virus) of VSV-TAP, the VSV-cDNA library (ASMEL), VSV-GFP ( $10^7$  pfu/injection), or PBS. The percentage of long term survivors (>60 days) for each treatment over three independent experiments is shown. **(b)** cDNA was initially inserted into the VSV genome pVSV-XN2 (ref. 23) between the *Xho1* and *Nhe1* cloning sites between the *G* and *L* genes. cDNA containing 5' and 3'UTR, the coding cDNA and the cellular poly A tail from human melanoma cells was initially cloned into the shuttle plasmid pSPORT6. These cDNA were transferred from the pSPORT6 plasmid into the pVSV-XN2 VSV genomic plasmid using PCR primers which recognized flanking pSPORT6 vector sequences (linker sequences) and the appropriate *Xho1* and *Nhe1* restriction sites. However, following virus production it was found that each of the immunogenic TAP was truncated at their C termini. **(c)** Schematic showing the sequencing results of each of the truncated VSV-TAP viruses from ASMEL. The terminal TAC tyrosine codon is converted to a TGA "stop" codon for each virus. **(d-f)** The C terminal sequences of the TAP found at the junction of cDNA and VSV sequences are shown for the **d** N-RAS, **e** CYT-C, and **f** TYRP-1 TAP. In each case the inserted cDNA sequence is *underlined*. In each case, a TAC codon (cDNA sequence, Tyrosine, Y) is mutated to TAG (STOP) converting a Tyrosine to a STOP (bolded); The 3' C terminal N-RAS amino acids deleted are YRMKLLNSDDGTQGCMGLPCVVM; the 3' C terminal CYT-C amino acid sequences deleted are YTIKRHKWSVLKSRKLAIRPPK; and the 3' C terminal TYRP-1 amino acids deleted are YQCYAEYEKLNPNQSVV. GCTAGC is the *Nhe1* site in the VSV genome in the intergenic region between the *G* and *L* genes; TATGAAAAA is the intergenic VSV polyA sequence (italicized); CT is the intergenic dinucleotide between the *G* and *L* genes of VSV (italicized); AACAG is the intergenic VSV transcription start sequence; and the final ATG is the start codon of the *L* gene. ASMEL, altered-self melanoma; PBS, phosphate buffered saline; PCR, polymerase chain reaction; TAP, tumor-associated proteins; VSV, Vesicular Stomatitis Virus.

## RESULTS

Therapeutically active cDNA expressed from VSV are truncated

Our previous work has shown that the combination of VSV-N-RAS, VSV-Cytochrome C, and VSV-TYRP1 (VSV-TAP) mimics most of the therapeutic effects of treatment with the altered-self melanoma (ASMEL) TAP library against established B16 mouse tumors (Figure 1a).<sup>16</sup> During the construction of the initial cDNA library, polyA-containing cellular cDNAs were cloned into the VSV genomic plasmid (pXN2)<sup>23</sup> using *Xho*1 and *Nhe*1 sites (Figure 1b). Sequencing of the cellular cDNA contained in the VSV-N-RAS, VSV-Cytochrome C, and VSV-TYRP1 revealed no mutations in the cDNA inserts. However, in each case, the cellular cDNA were truncated at their C-termini (Figure 1c). Although the deletions of the cellular sequences varied in length, the final amino acid that was lost in each case was a Tyrosine residue (TAC to TGA “stop” codon), which became juxtaposed with the first guanine of the *Nhe*1 cloning site (Figure 1d–f). In addition to the loss of the C-termini of the proteins, the deletions also removed the cellular 3'-untranslated (3'-UTR) and poly-A tails which were included from the initial method of cDNA library construction (Figure 1c).

Deletion of coding sequences and poly-A as a result of viral passage

To investigate the significance of these deletions in each of the VSV-TAP recovered from the initial library, we constructed a VSV expressing only the full length cDNA of the *N-RAS* gene<sup>24</sup> with no 3'UTR or cellular poly-A tail (VSV-cDNA-N-RAS) (Figure 2a). Following rescue of this virus from BHK cells, the full length *N-RAS* cDNA was retained through viral multiple passages (>10) as shown by polymerase chain reaction (PCR) (Figure 2b). Cells infected by the ASMEL VSV-cDNA library predominantly expressed the deleted *N-RAS* encoded for by VSV-Δ-N-RAS (Figure 2b). These data show that the full-length coding region of the *N-RAS* cDNA, without a poly-A tail and 3'UTR can be carried as a stable insert through multiple passages in VSV.

The parental pXN2-cDNA plasmid library (that was used to create the viral library) did not possess the 60 bp cDNA deletion found in the truncated VSV-Δ-N-RAS virus (Figure 2c,d). However, the sequence (linking the cDNA of *N-RAS* with the viral *L* gene) was deleted, including the 3'UTR region, in VSV recovered from cells infected with the ASMEL library (Figure 2c,d). This deletion also

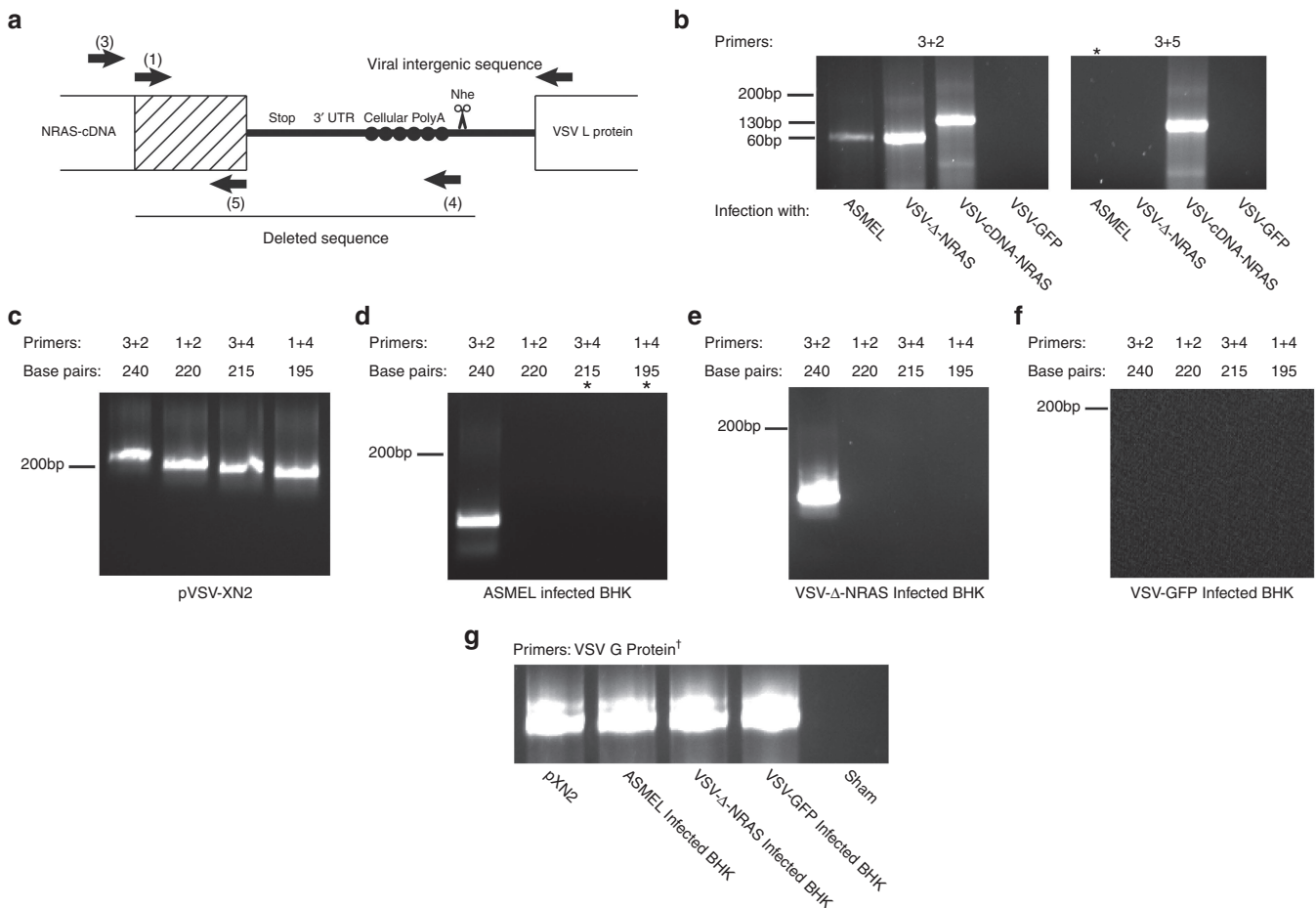


**Figure 2** Characterization of VSV-TAP truncations. **(a)** Schematic of VSV-cDNA-N-RAS generated showing original cloned product and deleted sequence. Location of primers used for diagnostic PCRs are shown (arrows). **(b)** PCR product from BHK cells infected with viruses shown (MOI 0.1, 48 hours postinfection) using the primer pairs shown. **(c)** PCR product from the plasmid pXN2-cDNA library, which was used to generate the ASMEL VSV-cDNA library stocks, or **(d)** from cDNA of BHK cells infected with the ASMEL VSV-cDNA library (MOI 0.1, 24 hours postinfection) using the primer pairs as shown. **(e)** PCR from cDNA of BHK cells infected with the VSV-Δ-N-RAS or **(f)** VSV-GFP viruses (MOI 0.1, 24 hours postinfection) using the primer pairs as shown. **(g)** PCR from the pXN2-cDNA plasmid library (100 ng), the viruses listed (MOI 0.1, 24 hours postinfection), or from sham infected BHK cells using VSV-G-specific primers. \*Indicates a signal obtained using 40 cycles of amplification; †Indicates a signal obtained using 10 cycles of amplification (all others were 25 cycles). The size of PCR products which are predicted from the primer pairs following PCR from a nondeleted viral genome as in **a** are shown (bp = base pairs). ASMEL, altered-self melanoma; GFP, green fluorescence protein; MOI, multiplicity of infection; PBS, phosphate buffered saline; PCR, polymerase chain reaction; TAP, tumor-associated proteins; VSV, Vesicular Stomatitis Virus.

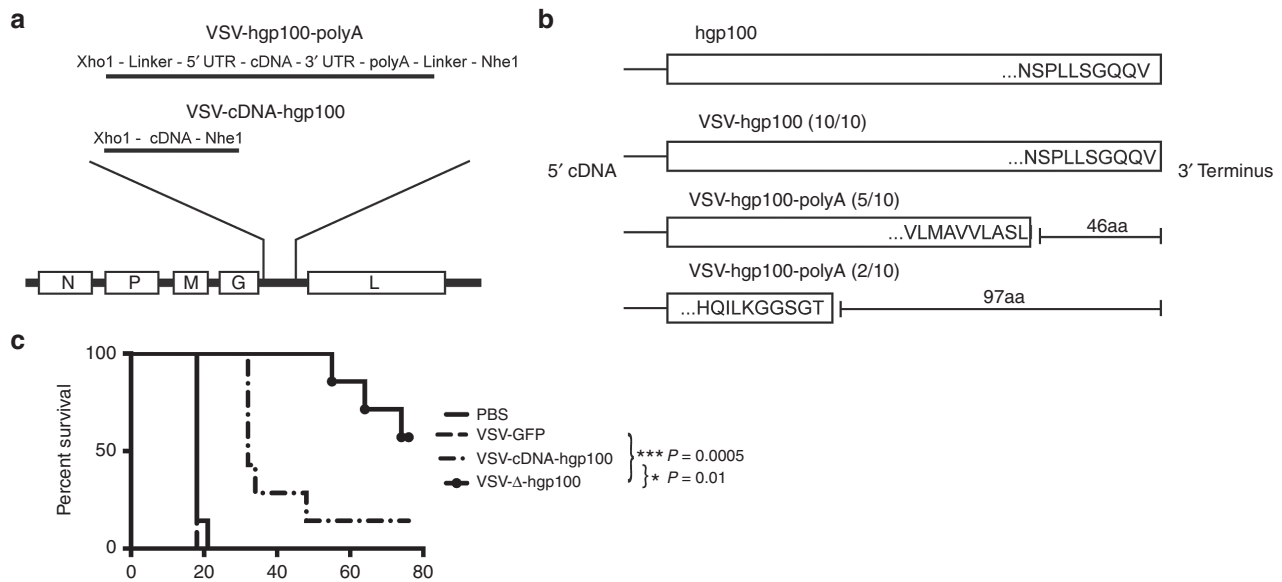


**Figure 3** Truncated hgp100 is a more potent antitumor therapeutic than the full-length hgp100. **(a)** The minimal cDNA of the human *gp100* gene (VSV-cDNA-hgp100), or the same cDNA with its associated cellular poly-A tail (VSV-hgp100-poly-A), were cloned into the pXN2 plasmid, from which the corresponding viruses were generated. **(b)** The VSV-hgp100 and VSV-hgp100-poly-A viruses were passaged through BHK cells three times (100  $\mu$ l of cell supernatants used to infect new BHK cells 48 hours following infection). About 10 plaques of each virus were picked and sequenced across the L and G genes. The number of plaques containing full-length or truncated proteins is shown along with the C-terminal amino acid sequence and the length of truncation. **(c)** Mice bearing 5-day-old established subcutaneous B16 tumors were treated ( $n = 7-8$ /group) as described in Figure 1 with the viruses shown ( $10^7$  pfu/injection) or PBS. Percent overall survival is shown. PCR, polymerase chain reaction; PBS, phosphate buffered saline; VSV, Vesicular Stomatitis Virus.

included the cellular poly-A tail and plasmid linker sequences. No PCR products linking N-RAS cDNA and VSV-L protein sequences were detected from cells infected with the control VSV-GFP virus and cDNA for the VSV-G envelope protein was abundant in all cells infected with VSV (Figure 2e-g). Therefore, the deletion seen in the VSV- $\Delta$ -N-RAS virus was not present in the plasmid cDNA library, but resulted from passage of virus through cells.

To test the hypothesis that truncation seen in VSV- $\Delta$ -N-RAS was a result of incompatibility between retention of the cellular poly-A tail and normal viral transcription, we constructed VSVs expressing the human melanoma antigen hgp100 cDNA<sup>25</sup> with, or without, a 3'UTR and a poly-A tail (Figure 3a). Following three passages of these viruses through BHK cells, 10 plaques of both viruses were isolated and sequenced. All of the VSV-hgp100 viruses expressing only the cDNA retained the full-length cDNA (Figure 3b). Half of the plaques from the serial passage of the VSV-hgp100-poly-A virus were truncated by 46 C terminal amino acids and two plaques were truncated by an additional 51 amino acids (Figure 3b). The remaining 3 out of 10 plaques did not provide informative sequence. As in Figure 1 both truncations resulted in the generation of a new TGA stop codon that became juxtaposed with the *Nhe1* site in the viral genome. Therefore, in two separate examples (VSV-N-RAS and VSV-hgp100), multiple passages of a VSV-cDNA virus including a cellular poly-A tail led to its deletion and truncation of the encoded cDNA.

#### Therapeutic consequences of 3' protein truncations

Intravenous injection of nine doses of VSV- $\Delta$ -hgp100 (46 amino acids deleted, generated from Figure 3b) was significantly more therapeutic against 5 day established B16 tumors than either VSV-cDNA-hgp100 (not truncated) ( $P = 0.0137$ ) or VSV-GFP ( $P = 0.0005$ ) (Figure 3c).

We also engineered VSV expressing only the cDNA of the *TYRP-1* (ref. 26) or *CYT-C* (ref. 27) genes, with no 3'UTR or poly-A tail like the VSV-cDNA N-RAS described above. Together we will refer to these

three viruses as VSV-cDNA-TAP. As described previously, between 70-80% of mice with established 5 day B16 tumors were cured of their tumors by intravenous injection of nine doses of VSV- $\Delta$ -TAP (two separate experiments shown in Figure 4a-d). Although there was a significant prolongation of survival of mice treated with the combination of VSV-cDNA-TAP compared with sham treated mice ( $P = 0.0013$ ), only a single mouse had a durable response in the experiment of Figure 4a. Consistent with our previous findings<sup>15,16</sup> and *in vitro* findings, *in vivo* depletion showed that the therapeutic effects of VSV- $\Delta$ -TAP were completely dependent upon CD4+ T cells, and, to a lesser extent, also dependent upon CD8+ T cells (Figure 4e). In contrast, depletion of CD8+ T cells completely abrogated the therapy of VSV-cDNA-TAP and CD4+ T cell depletion had no significant effect on therapy (Figure 4f).

#### Truncated cDNA are also immunogenic in plasmid vectors

Finally, we investigated whether truncated cDNA were more immunogenic than full-length counterparts when expressed from another vector platform. The cDNA library used to create the ASMEI was initially cloned into a plasmid in which the CMV promoter drives expression of the full-length cDNA (pcDNA) (Figure 5a). PCR confirmed that the cDNA in this plasmid library were full length before being cloned into the VSV genome (Figure 2). We also generated a plasmid vector encoding truncated cDNA (p $\Delta$ cDNA) by cloning the full range of truncated cDNA, as expressed from the ASMEI, using real-time PCR from BHK cells infected by the VSV-cDNA library (Figure 5a). Truncation of individual cDNA (N-RAS and CYT-C), as they were expressed from the VSV-cDNA library (Figure 2), was confirmed by PCR (not shown).

Intradermal injections of either pcDNA or p $\Delta$ cDNA into tumor bearing mice had no significant effect on tumor control (not shown). In contrast, the addition of CpG as an adjuvant to these plasmid injections uncovered significant antitumor activity of both

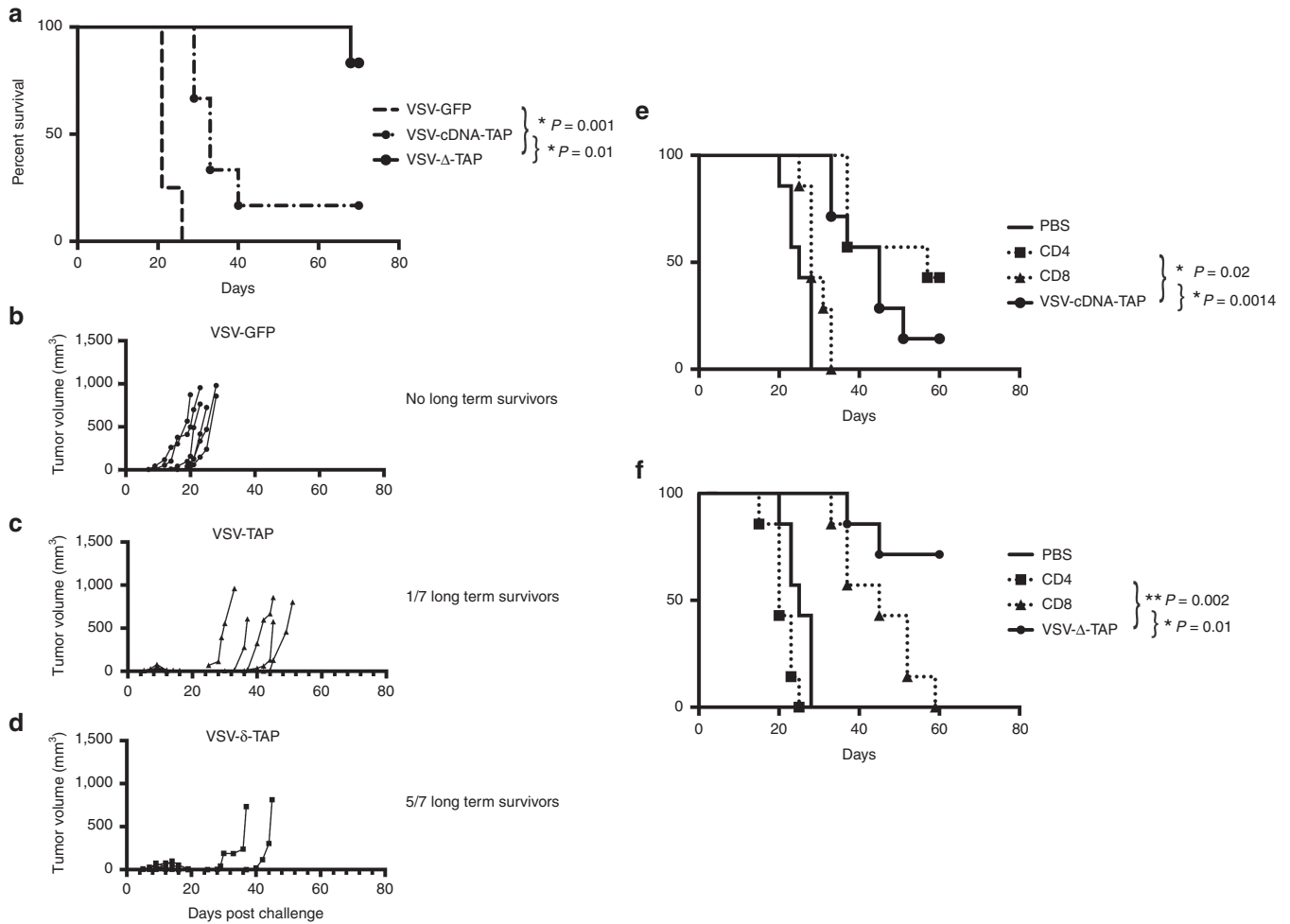


**Figure 4** Truncated self-TAP generate long-lived protective antitumor therapy. (a) Mice bearing 5-day-old established s.c. B16 tumors were treated ( $n = 7-8$ /group) with nine i.v. injections as in Figure 1 with the viruses shown. Survival with time is shown. (b-d) Mice bearing 5-day-old s.c. B16 tumors were treated with nine i.v. injections on days 6-8, 13-15, and 20-22 with **b** VSV-GFP ( $10^7$  pfu/injection), **c** VSV-cDNA-TAP (a three-way combination, total viral dose  $10^7$  pfu/injection; and  $3 \times 10^6$  pfu of each virus) or with **d** VSV-Δ-TAP. Tumor volumes with time are shown. In general, tumors became palpable and either progressed without regression (VSV-GFP); plateaued and regressed with a later recurrence (VSV-cDNA-TAP, VSV-Δ-TAP) or plateaued, regressed and remained undetectable for the duration of the experiment (VSV-Δ-TAP). The experiment of **a** above was repeated, by treating 5-day-tumor bearing mice with (e) VSV-cDNA-TAP or (f) VSV-Δ-TAP with, or without, the depletion of CD8+ cells or CD4+ cells. GFP, green fluorescence protein; TAP, tumor-associated proteins; VSV, Vesicular Stomatitis Virus.

pcDNA and pΔcDNA (compared with pCMV-GFP + CpG) (Figure 5b). However, pΔcDNA + CpG was significantly better at prolonging survival than pcDNA + CpG (Figure 5b), confirming that antitumor immunity can be manipulated through the integrity of the proteins expressed from vectors other than just VSV.

## DISCUSSION

Here, we show that VSV-mediated expression of truncated versions of otherwise normal self-proteins leads to a CD4+ T cell dependent immune response which is highly effective at rejecting established tumors. These findings will have considerable significance for the design of more effective cancer vaccines where the goal is to break tolerance to normal self-TAP.<sup>28,29</sup>

We built upon our previous observation that a combination of three different self-proteins, expressed from VSV was necessary and sufficient to generate rejection of established B16 tumors in C57BL/6 mice (Figure 1a). Sequencing of the inserts of these immunogenically active viruses, compared with the parent plasmids from which the virus library was made, revealed that each one encoded

a truncated version of the normal protein and that this truncation was not a result of the molecular construction of the library in the plasmid (Figure 2). The normal mechanism of VSV gene expression involves polymerase detachment mediated by viral poly-A tails followed by reinitiation between coding sequences.<sup>30,31</sup> We have shown here that if a cellular poly-A tail is included in the transgene cloned into VSV (either multiple cDNA or hgp100), it is excised at high frequency from replicating clones of the virus. Our current hypothesis is that the viral polymerase interacts with the human poly-A tail in some way that promotes premature detachment from the viral template and interferes with the reattachment necessary to initiate transcription of the downstream (*L*) viral gene. However, exactly what the properties of the cellular poly-A tail sequences are that cause them to be so strongly selected against in replicating VSV remain to be elucidated. Consistent with this hypothesis, *in vitro* passage of the VSV-hgp100-poly-A virus generated progeny viruses in which the cDNA was truncated, with loss of the associated cellular poly-A tails. In contrast, passage of the VSV-cDNA-hgp100 (no cloned poly-A), virus did not generate any truncations of the cDNA (Figure 3). We are currently investigating the mechanisms of how

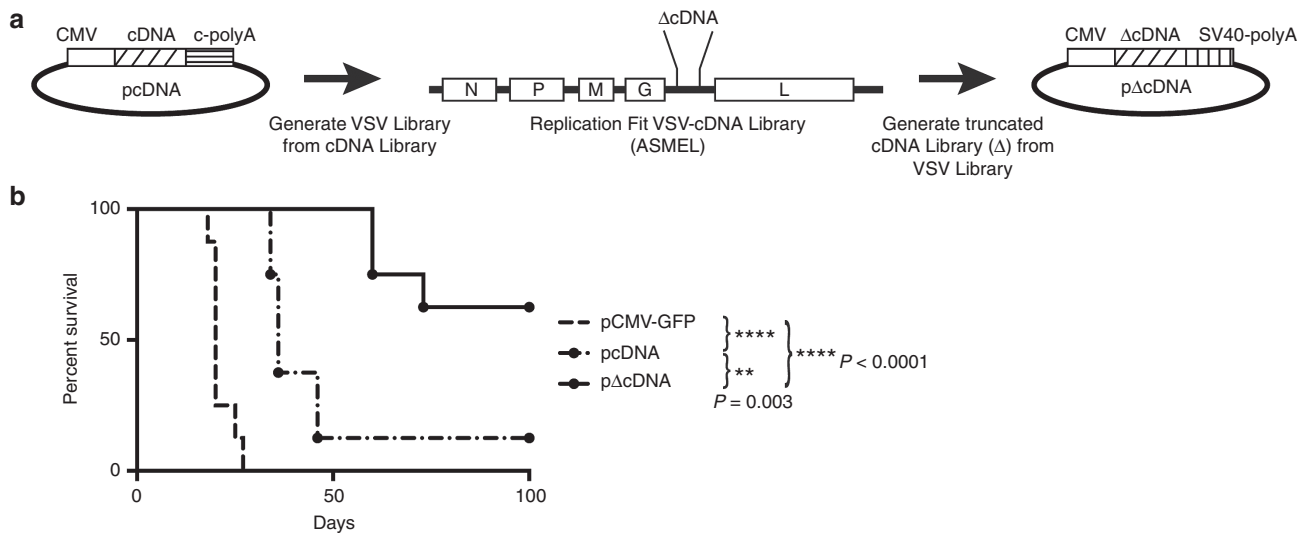


**Figure 5** Immunogenicity of truncated cDNA in plasmid vectors. **(a)** cDNA from 2 human melanoma cell lines was cloned into a CMV-expression vector to generate a plasmid cDNA library which included full length cDNA clones along with the cellular poly A (CpolyA). cDNA in this plasmid library (pcDNA) was confirmed to be nontruncated (Figure 2). This library was cloned into the VSV genomic plasmid pXN2, as previously described<sup>16,17</sup> to generate the VSV library (ASMEL). Following passage through BHK cells, the now truncated cDNA library was cloned back into the parental plasmid using RT-PCR to generate the truncated plasmid library (pΔcDNA). The truncated cDNA were expressed from the plasmid using the SV40 poly A as shown. **(b)** Mice bearing 5-day-old established s.c. B16 tumors were treated ( $n = 7-8/\text{group}$ ) with nine intradermal injections of pCMV-GFP, pcDNA, or pΔcDNA (10  $\mu\text{g}$  plasmid per injection) with 100  $\mu\text{g}$  CpG per injection on days 6, 8, 10, 13, 15, 17, 20, 22, and 24. Survival of treated mice with time is shown. Groups were compared using the log rank test. (\*\* $P < 0.01$ , \*\*\*\* $P < 0.0001$ , n.s. = not significant.) Reprinted from refs. 16, 17 possibly with permission of publisher or organization. ASMEL, altered-self melanoma; GFP, green fluorescence protein; RT-PCR, reverse transcriptase polymerase chain reaction; TAP, tumor-associated proteins; VSV, Vesicular Stomatitis Virus.

this deletion occurs. The repeated finding that the deletion is associated with a tyrosine residue suggests that recombination at specific bases within the cDNA coding sequence is important. Therefore, the method by which we initially constructed the cDNA library in VSV, by inclusion of cellular poly-A tails, led fortuitously to the emergence of VSV-encoded self-TAP as truncated versions of the normal self-proteins.

We have shown in previous reports that both VSV-cDNA library and VSV-Δ-TAP therapy are dependent upon CD4+ T cells.<sup>15-18</sup> Our data in Figure 4 are consistent with these findings, demonstrating that truncated and full length self-proteins skew the resultant antitumor immune response toward CD4+ T cell dependent (truncated) or CD8+ T cell dependent (full length) responses (Figure 4). Although the same titers of VSV expressing full length and truncated versions of each TAP were used, we cannot exclude that differences in levels of TAP expression may occur *in vivo* in APC stimulated to present the different TAP. If so, expression levels may influence levels of TAP presentation and ultimate immunogenicity.

With either VSV- or plasmid- mediated delivery of truncated versions of normal self-TAP an intensive schedule of vaccination was required (nine i.v. injections of VSV or addition of CpG adjuvant). We believe that the adjuvant activity of the innate immune activation induced by the VSV or CpG has dual anti-tumor effects. Systemic activation of innate immune effectors through VSV- or CpG- mediated TLR activation can lead to initial control of tumor growth consistent with our previous findings that VSV oncolytic therapy of B16 tumors requires innate immune effectors and Myd88 signaling.<sup>32,33</sup> In addition, TLR activation leads to potent activation of APC in the lymph nodes in the presence of the codelivered TAP. The result is the combination of potent innate immune effector activation along with the priming of relatively weak antitumor T cell responses against self-TAP which are together able to clear established tumors.

Our current results also extend our previous work to show that this CD4+ T cell dependent response raised against truncated self-TAP was significantly more therapeutically potent than the CD8+ T cell dependent response raised against the corresponding full length self-TAP. In some respects, the superiority of the CD4+ T cell response against truncated antigens over the CD8+ T cell response against full length antigens appears to be counterintuitive. However, these results are consistent with reports that several types of autoimmune responses are often closely associated with CD4+ T cells.<sup>34,35</sup> Since the antigenic targets against which antitumor immune responses are directed here are all derivatives of self-proteins, these antitumor responses are essentially autoimmune. Overall, these data suggest that strategies aimed at raising potent autoimmune, CD4+ T cell dependent responses should be developed along with those targeting more classical CD8+ T cell activation, especially when the antigenic targets are essentially self-proteins.

Taken together, our data show that the type and potency of antitumor immune responses against self-TAP can be manipulated *in vivo* through the integrity of the self protein that is used (full length or truncated self-TAP) and the resultant skewing of the T cell response to either a CD8+ or a CD4+ phenotype. These results have broad and important implications for the future design of cancer vaccines used alone or in combination with further immune potentiators such as checkpoint inhibitors.<sup>3-5</sup> Thus, we have shown that vaccines in which self-TAP are intentionally truncated may be significantly more potent than those using full length proteins and that the enhanced immunogenicity of these truncated proteins is not dependent upon the type of vector used (Figures 4 and 5). We are currently investigating the molecular basis of the different antitumor immune responses raised by truncated versus full-length self-proteins. In this respect, one possible hypothesis is that this increased immunogenicity is associated with the activation of the UPR by these truncated, and therefore, likely to be poorly folded proteins.<sup>7-10</sup> VSV infection itself will activate

the UPR and so additional activation by poorly folded proteins may accentuate the immunogenicity of virally encoded TAP through directing appropriate epitopes into different pathways of antigen presentation and/or by triggering production of inflammatory cytokines. In addition, other pathways, such as the nonsense mediated decay (NMD)-pathway may also be responsible for the altered antigen-presentation of these truncated self-proteins. It may also be observed that deletion of C terminal sequences of the TAP leads to the loss of important epitopes which mediate suppressive anti-TAP T cell responses.

This represents a new area for exploitation in the design of cancer vaccines, in which generation of self-TAP immunogens based upon alterations in protein integrity may be complementary to those approaches based upon changes in neo-antigen expression and sequence mutation.<sup>3-5</sup> Finally, our data here may have considerable significance for understanding the etiology of autoimmune diseases in which pathogen infection, stress, or trauma may activate the UPR, thereby triggering responses against self-antigen leading to autoimmune pathologies.<sup>19-22</sup>

## MATERIALS AND METHODS

### Cells and viruses

Murine B16 F1 melanoma (H2-K<sup>b</sup>) cells (American Type Culture Collection, Manassas, VA) were maintained as previously described and grown in Dulbecco's modified Eagle's medium (DMEM; Life Technologies, Carlsbad, CA) supplemented with 10% (v/v) fetal calf serum (FCS; Life Technologies) and L-glutamine (Life Technologies). All cell lines were routinely monitored and found to be free of *Mycoplasma* infection.

VSV-cDNA libraries were generated as previously described.<sup>15,16</sup> Briefly, cDNA from human melanoma cell lines were pooled and cloned into the pCMV.SPORT6 cloning vector (Invitrogen, Carlsbad, CA) and amplified by PCR. The cDNA were then size fractionated to below 4 kbp for ligation into the parental VSV genomic plasmid, pVSV-XN2 (ref. 23), between the G and the L genes. Virus was generated from BHK cells by cotransfection of pVSV-XN2-cDNA library DNA along with plasmid encoding viral genes as described.<sup>23</sup> Virus was expanded by infection of BHK cells and purified by sucrose gradient centrifugation.

VSV expressing individual cDNA (with or without the 3'UTR and poly-A tail of the gene) were generated by cloning the cDNA into the plasmid pVSV-XN2, as described.<sup>15,16,23</sup> Monoclonal VSV-cDNA were obtained by plaque purification on BHK-21 cells. Concentration and purification were done by sucrose gradient centrifugation. Titers were measured by standard plaque assays on BHK-21 cells.<sup>23</sup>

### In vivo studies

All procedures were approved by the Mayo Foundation Institutional Animal Care and Use Committee. C57BL/6 mice were purchased from Jackson Laboratories (Bar Harbor, ME) at 6–8 weeks of age. To establish subcutaneous tumors,  $2 \times 10^5$  B16 cells in 100  $\mu$ l of phosphate buffered saline (PBS) were injected into the flank of mice. Typically, these tumors became palpable within 5–7 days. For *in vivo* treatment protocols, C57BL/6 mice bearing 5-day-old s.c. B16 tumors were treated (typically  $n = 7-8$ /group) with nine i.v. injections on days 6–8, 13–15, and 20–22 of the viruses as described in the text. Total viral doses of  $10^7$  pfu/injection were used in 100  $\mu$ l. For survival studies, tumor diameter in two dimensions was measured three times weekly using calipers and mice were killed when tumor size was  $\sim 1.0 \times 1.0$  cm in two perpendicular directions.

Immune cell depletions were done by intraperitoneal injections (0.1 mg per mouse) of anti-CD8 (Lyt 2.43), anti-CD4 (GK1.5), both from the Monoclonal Antibody Core Facility, Mayo Clinic; and IgG control (ChromPure Rat IgG, Jackson ImmunoResearch, West Grove, PA) at day 4 after tumor implantation and weekly thereafter.

### Reverse transcriptase PCR

RNA was prepared from cell cultures with the Qiagen (Hilden, Germany) RNA extraction kit. About 1  $\mu$ g total cellular RNA was reverse transcribed in a 20  $\mu$ l volume using oligo-(dT) as a primer. A cDNA equivalent of 1 ng RNA was amplified by PCR with gene specific primers.

## Statistics

Survival data from the animal studies were analyzed using the log rank test. All statistical analysis was carried out in GraphPad Prism software (GraphPad Software, La Jolla, CA). Statistical significance was determined at the level of  $P < 0.05$ .

## CONFLICT OF INTEREST

The authors declared no conflict of interest.

## ACKNOWLEDGMENTS

The authors thank Toni L. Woltman for expert secretarial assistance. This work was funded in part by The European Research Council, The Richard M. Schulze Family Foundation, the Mayo Foundation, Cancer Research, UK, the National Institutes of Health (R01CA175386, R01CA108961), the University of Minnesota, and Mayo Clinic Partnership and also a grant from Terry and Judith Paul. S.Z. and KH acknowledge support from the ICR/RM NIH Biomedical Research Centre. K.S. acknowledges support from Mayo Clinic Medical Scientist Training Program through the National Institute of General Medical Sciences (T32 GM65841).

## REFERENCES

1. Rosenberg, SA and Restifo, NP (2015). Adoptive cell transfer as personalized immunotherapy for human cancer. *Science* **348**: 62–68.
2. Sadelain, M (2015). CAR therapy: the CD19 paradigm. *J Clin Invest* **125**: 3392–3400.
3. Topalian, SL, Drake, CG and Pardoll, DM (2015). Immune checkpoint blockade: a common denominator approach to cancer therapy. *Cancer Cell* **27**: 450–461.
4. Coulie, PG, Van den Eynde, BJ, van der Bruggen, P and Boon, T (2014). Tumour antigens recognized by T lymphocytes: at the core of cancer immunotherapy. *Nat Rev Cancer* **14**: 135–146.
5. Gubin, MM, Artyomov, MN, Mardis, ER and Schreiber, RD (2015). Tumor neoantigens: building a framework for personalized cancer immunotherapy. *J Clin Invest* **125**: 3413–3421.
6. Tran, E, Ahmadzadeh, M, Lu, YC, Gros, A, Turcotte, S, Robbins, PF *et al.* (2015). Immunogenicity of somatic mutations in human gastrointestinal cancers. *Science* **350**: 1387–1390.
7. Cláudio, N, Dalet, A, Gatti, E and Pierre, P (2013). Mapping the crossroads of immune activation and cellular stress response pathways. *EMBO J* **32**: 1214–1224.
8. Hetz, C, Chevet, E and Oakes, SA (2015). Proteostasis control by the unfolded protein response. *Nat Cell Biol* **17**: 829–838.
9. Tameire, F, Verginadis, II and Koumenis, C (2015). Cell intrinsic and extrinsic activators of the unfolded protein response in cancer: Mechanisms and targets for therapy. *Semin Cancer Biol* **33**: 3–15.
10. Zanetti, M, Rodvold, JJ and Mahadevan, NR (2016). The evolving paradigm of cell-nonautonomous UPR-based regulation of immunity by cancer cells. *Oncogene* **35**: 269–278.
11. Janssens, S, Pulendran, B and Lambrecht, BN (2014). Emerging functions of the unfolded protein response in immunity. *Nat Immunol* **15**: 910–919.
12. Schwab, SR, Shugart, JA, Horng, T, Malarkannan, S and Shastri, N (2004). Unanticipated antigens: translation initiation at CUG with leucine. *PLoS Biol* **2**: e366.
13. Kaluza, KM, Kottke, T, Diaz, RM, Rommelfanger, D, Thompson, J and Vile, R (2012). Adoptive transfer of cytotoxic T lymphocytes targeting two different antigens limits antigen loss and tumor escape. *Hum Gene Ther* **23**: 1054–1064.
14. Mittal, D, Gubin, MM, Schreiber, RD and Smyth, MJ (2014). New insights into cancer immunoediting and its three component phases—elimination, equilibrium and escape. *Curr Opin Immunol* **27**: 16–25.
15. Kottke, T, Errington, F, Pulido, J, Galivo, F, Thompson, J, Wongthida, P *et al.* (2011). Broad antigenic coverage induced by vaccination with virus-based cDNA libraries cures established tumors. *Nat Med* **17**: 854–859.
16. Pulido, J, Kottke, T, Thompson, J, Galivo, F, Wongthida, P, Diaz, RM *et al.* (2012). Using virally expressed melanoma cDNA libraries to identify tumor-associated antigens that cure melanoma. *Nat Biotechnol* **30**: 337–343.
17. Alonso-Camino, V, Rajani, K, Kottke, T, Rommelfanger-Konkol, D, Zaidi, S, Thompson, J *et al.* (2014). The profile of tumor antigens which can be targeted by immunotherapy depends upon the tumor's anatomical site. *Mol Ther* **22**: 1936–1948.
18. Boisgerault, N, Kottke, T, Thompson, J, Diaz, RM, Rommelfanger-Konkol, D *et al.* (2013). Functional cloning of recurrence-specific antigens identifies molecular targets to treat tumor relapse. *Mol Ther* **21**: 1507–1516.
19. Cao, SS, Luo, KL and Shi, L (2016). Endoplasmic reticulum stress interacts with inflammation in human diseases. *J Cell Physiol* **231**: 288–294.

20. Hetz, C, Chevet, E and Harding, HP (2013). Targeting the unfolded protein response in disease. *Nat Rev Drug Discov* **12**: 703–719.
21. Park, H, Bourla, AB, Kastner, DL, Colbert, RA and Siegel, RM (2012). Lighting the fires within: the cell biology of autoinflammatory diseases. *Nat Rev Immunol* **12**: 570–580.
22. Stone, S and Lin, W (2015). The unfolded protein response in multiple sclerosis. *Front Neurosci* **9**: 264.
23. Fernandez, M, Porosnicu, M, Markovic, D and Barber, GN (2002). Genetically engineered vesicular stomatitis virus in gene therapy: application for treatment of malignant disease. *J Virol* **76**: 895–904.
24. Hall, A and Brown, R (1985). Human N-ras: cDNA cloning and gene structure. *Nucleic Acids Res* **13**: 5255–5268.
25. Adema, GJ, de Boer, AJ, Vogel, AM, Loenen, WA and Figdor, CG (1994). Molecular characterization of the melanocyte lineage-specific antigen gp100. *J Biol Chem* **269**: 20126–20133.
26. Shibata, K, Takeda, K, Tomita, Y, Tagami, H and Shibahara, S (1992). Downstream region of the human tyrosinase-related protein gene enhances its promoter activity. *Biochem Biophys Res Commun* **184**: 568–575.
27. Suzuki, H, Hosokawa, Y, Nishikimi, M and Ozawa, T (1989). Structural organization of the human mitochondrial cytochrome c1 gene. *J Biol Chem* **264**: 1368–1374.
28. Lizée, G, Overwijk, WW, Radvanyi, L, Gao, J, Sharma, P and Hwu, P (2013). Harnessing the power of the immune system to target cancer. *Annu Rev Med* **64**: 71–90.
29. Pardoll, D (2015). Cancer and the immune system: basic concepts and targets for intervention. *Semin Oncol* **42**: 523–538.
30. Ball, LA, Pringle, CR, Flanagan, B, Perepelitsa, VP and Wertz, GW (1999). Phenotypic consequences of rearranging the P, M, and G genes of vesicular stomatitis virus. *J Virol* **73**: 4705–4712.
31. Rose, JK, and Whitt, MA (2001). *Rhabdoviridae: The Viruses and Their Replication*. 4th ed. Lippincott Williams and Wilkins: New York. pp. 1221–1243.
32. Wongthida, P, Diaz, RM, Galivo, F, Kottke, T, Thompson, J, Melcher, A *et al.* (2011). VSV oncolytic virotherapy in the B16 model depends upon intact MyD88 signaling. *Mol Ther* **19**: 150–158.
33. Wongthida, P, Diaz, RM, Galivo, F, Kottke, T, Thompson, J, Pulido, J *et al.* (2010). Type III IFN interleukin-28 mediates the antitumor efficacy of oncolytic virus VSV in immune-competent mouse models of cancer. *Cancer Res* **70**: 4539–4549.
34. Gaffen, SL, Jain, R, Garg, AV and Cua, DJ (2014). The IL-23-IL-17 immune axis: from mechanisms to therapeutic testing. *Nat Rev Immunol* **14**: 585–600.
35. Patel, DD and Kuchroo, VK (2015). Th17 cell pathway in human immunity: lessons from genetics and therapeutic interventions. *Immunity* **43**: 1040–1051.



This work is licensed under a Creative Commons Attribution-NonCommercial-NoDerivs 4.0 International License. The images or other third party material in this article are included in the article's Creative Commons license, unless indicated otherwise in the credit line; if the material is not included under the Creative Commons license, users will need to obtain permission from the license holder to reproduce the material. To view a copy of this license, visit <http://creativecommons.org/licenses/by-nc-nd/4.0/>

© The Author(s) (2016)